Modeling of the Reinforcement Minimum Spacing of Precast Concrete Using Grouting

Anis Rosyidah[1]
[1]*Civil Engineering*
Politeknik Negeri Jakarta
Depok, Indonesia
[1]anis.rosyidah@sipil.pnj.ac.id

Gigih Muslim Prayogo[2]
[2]*Civil Engineering*
Politeknik Negeri Jakarta
Depok, Indonesia
[2]gigihmuslim@gmail.com

I Ketut Sucita[3]
[3]*Civil Engineering*
Politeknik Negeri Jakarta
Depok, Indonesia
[3]cita.sandi@gmail.com

***Abstract*— The pull-out test of precast concrete connection system using grouting to find the characteristics and behavior of the connection system in resisting axial tensile forces. Besides experiments in the laboratory, it can also be simulated modeling using software Finite Element Method. The specimens modeling on the pullout test in this study used four bars, there are two rows and two columns configuration. The compression strength of concrete is 25, and 35 MPa and the grouting use Masterflow 810. The purpose of this modeling is to find the minimum distance of reinforcement required to avoid a collapse in concrete and grouting. The bars diameter is D16, D19, D22, D25, and D28. The bars spacing are 1.5D, 2D, 2.5 D, 3D, 3.5D, 4D also 5D, where D is the outer diameter of the grouting thickness of 2 times bars diameter. The constitutive modeling is using concrete damage plasticity theory. It is to identify the pattern of failure of the specimens. The results showed that the greater of bars spacing, the smaller the percentage of element failure. Concrete and grouting material damaged by tensile stress, where the most significant failure at 1.5D length about 15% -25% and the grouting element of 78% -95%. Recommendation of bars minimum distance to prevent the failure in concrete and grouting that is equal to 4D.**

Keywords*— *Pullout Test, Bars Minimum Spacing, Finite Element Method, Concrete Damage Plasticity

I. INTRODUCTION

The use of precast concrete is more environmentally friendly compared to the conventional system of the cast in situ. The results show that carbon emissions produced by precast concrete are 10% lower per 1 m^3 of concrete. Moreover, the use of reinforcement (bars) is better planned, and the working methods can save molds and scaffoldings as well as can make the working area cleaner [1], [2].

The problem of precast concrete is the connection. In an ideal condition, the association should have similar properties with conventional concrete. The effort to get identical connection conditions to conventional concrete has developed rapidly, for examples male and female connection, at which one of the components of precast concrete is provided some space as a place for the bars which is covered by grouting. Grouting proven that it could implant the reinforcement in the concrete, as long as the length of the implanted reinforcement should suffice so that those connections would have the same bond strength as the monolithically casted concrete [3].

Grouted splice sleeve can also be used as the precast connections [4],[5]. Metal cartridge is installed to place the reinforcement (bars), then the round is filled with grouting [6]. This connection has excellent ability in accepting the monotonic and cyclic loads. The length of the canal needed for this connection is between 6.5 db up to 10db [7].

Grout pocket – double line pocket type of precast connection has a minimum length canal of 12db. The minimum distance between reinforcement bars in this connection is 2.5 db. What the kind of the failure occurred in the connection system is a failure to the concrete [8].

In the previous study on a precast connection using grouting concrete, a discussion of the distance between the longitudinal reinforcement has not reviewed, whereas the distance of this reinforcement contributes to the failure scheme. With the approach of finite element, this paper discusses the gap of the longitudinal reinforcement and failure scheme occurred on a concrete precast connection using grouting.

II. RESEARCH METHODS

Within one specimen, the number of reinforcement bars used in the modeling was four pieces. Steel bars used 400 Mpa of tensile strength. The concrete compressive strength used in modeling were 25 and 35. Grouting used Masterflow 810 with compressive strength ultimately ± 65 MPa.

Pull out the test method is presented in Fig. 1. The development length and the thickness of grouting used were similar sizes to all reinforcement bars diameter which was 20D and 2D.

The diameter of the reinforcement bars were D16, D19, D22, D25, and D28. The distance between reinforcement was 3.5D and 4D, as D was the outer diameter of grouting. This study also built the modeling using monoliths specimen (without grouting).

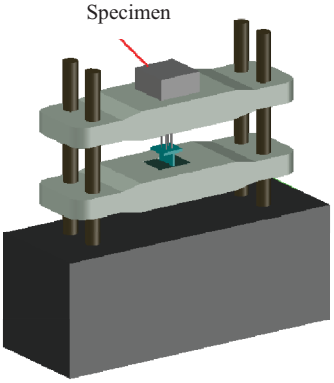

***Fig. 1** Pullout Test*

A. Model Approach

The modeling used in this study is Concrete Damage Plasticity (CDP) model [9], [10], [11]. This modeling concept combines the elasticity of the isotropic failure with isotropic tensile strength also with plasticity compressive strength to model the behavior of the concrete [12], [13]. The CDP modeling assumes scalar damage (isotropic) and can be used for either monotonic or cyclic load. The CDP modeling could be an effective method to analyze the behavior of plasticity concrete on tensile strength and compressive strength [14].

The behavior of uniaxial strain stress concrete used in the CDP modeling formulated by Lubliner [15] then modified and renewed by Lee and Fenves [16]. The function of this analysis combines two forms of the geometry of the Drucker-Prager function which shown in Figure 2; the purpose is also the basic modeling of Concrete Damage Plasticity on software.

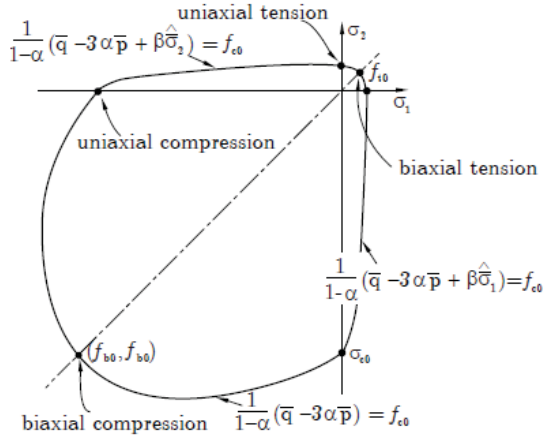

Fig. 2 Diagram of Biaxial Strain-Stress Concrete in Constitutive Concrete Damage Plasticity Modeling [17]

1. Modeling Parameters CDP

Several parameters to input in software in the CDP modeling are the elasticity modulus (Ec), poison ratio (μ), dilation angle (ψ), eccentricity (ϵ), ratio σ_{b0}/σ_{c0} and Kc. Dilation angle or dilation corner is the ratio of the percentage of the increase in vertical shear strain and increasing strain. Eccentricity is the result of composing a base diagram formulas of stress-strain of compressive test results on uniaxial concrete. The σ_{b0}/σ_{c0} ratio is the ratio of the initial equiaxial yield stress with initial uniaxial yield stress. Kc is the ratio between the second form of invariant stress on the tensile meridian and compressive meridian [18]. The number input to the software can be seen in Table 1.

Table 1 Parameter of CDP fc25, fc35 Concrete and Grouting Masterflow 810

Material	f'c (MPa)	ft (MPa)	Ec	u	Dilation Angle	Eccentricity	fb0/fc0	K
fc25	25	2.6	23650	0.2	38	0.1	1.76	0.7
fc35	35	3.2	27983	0.2	38	0.1	1.64	0.7
Masterflow 810	65	4.5	38134	0.2	38	0.1	1.46	0.7

2. Strain Stress of Tensile Uniaxial and Compressive Uniaxial

The data on strain stress of compressive uniaxial (Table 2) used in this modeling (eq. (1) & (2)) which was formulated by Popovic [19], whereas the data on strain stress of tensile uniaxial used in tension stiffening modeling which was discussed (Fig. 3) [17].

Table 2 Strain Stress and Parameter of fc25, fc35 Concrete Damage and Grouting Masterflow 810

σ (Yield Stress)			ε (Crushing Strain)			d_c (Damage Comp.)		
fc25	fc35	Masterfow 810	fc25	fc35	Masterfow 810	fc25	fc35	Masterfow 810
12.50	17.50	32.50	0	0	0	0	0	0
17.77	26.28	46.21	0.0008	0.0011	0.0013	0	0	0
21.92	29.99	57.00	0.0011	0.0014	0.0018	0	0	0
24.27	33.27	63.10	0.0014	0.0018	0.0023	0	0	0
25.00	35.00	65.00	0.0024	0.0025	0.0034	0	0	0
23.93	34.20	62.21	0.0029	0.0031	0.0042	0.043	0.023	0.043
21.63	30.98	56.24	0.0036	0.0041	0.0054	0.135	0.115	0.135
18.99	27.64	49.38	0.0044	0.0051	0.0067	0.240	0.210	0.240
16.46	23.74	42.78	0.0054	0.0064	0.0082	0.342	0.322	0.342
14.26	20.66	37.07	0.0065	0.0077	0.0098	0.430	0.410	0.430
12.40	16.66	32.25	0.0077	0.0099	0.0116	0.504	0.524	0.504
10.84	16.23	28.18	0.0089	0.0102	0.0135	0.566	0.536	0.566
9.52	12.63	24.76	0.0103	0.0134	0.0156	0.619	0.639	0.619
5.31	8.83	17.83	0.0189	0.0195	0.0220	0.788	0.748	0.726
3.36	6.10	13.20	0.0300	0.0285	0.0300	0.866	0.826	0.797

$$\sigma = \frac{\varepsilon}{\varepsilon_{cu}} . \frac{n.f_{cu}}{(n-1)+\left(\frac{\varepsilon}{\varepsilon_{cu}}\right)^2} \quad (1)$$

$$\frac{\frac{E_c}{f_{cu}}}{\varepsilon_{cu}} = \frac{n}{n-1} \quad (2)$$

With σ = concrete stress, ε = concrete strain, ε_{cu} : an ultimate concrete strain, n = coefficient of curve shape, and: ultimate of concrete stress.

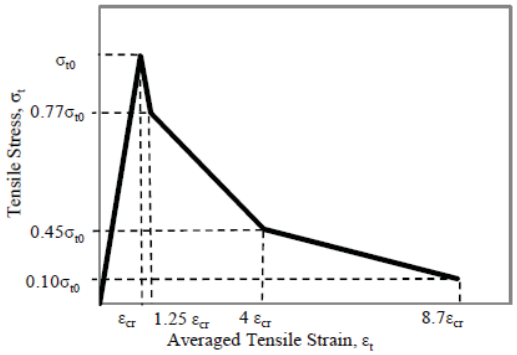

Fig. 3 Tension Stiffening Modeling at ABAQUS Manual (2008)

3. Modeling Interaction

Modeling on this specimen has four contacted surfaces that need to be defined for types of interaction. There are two interactions between surfaces in this modeling. They are concrete-grouting and reinforcement-grouting. The interaction between the concrete surfaces with grouting uses constraint-tie type. This type of interaction functions to bind a separate surface so that there is no relative movement between the covers. The reinforcement-grouting surface uses mechanical interaction in the form of friction with the

friction coefficient of 0.3. The specimen dimensions in this study can be seen in Fig. 4 and Table 3.

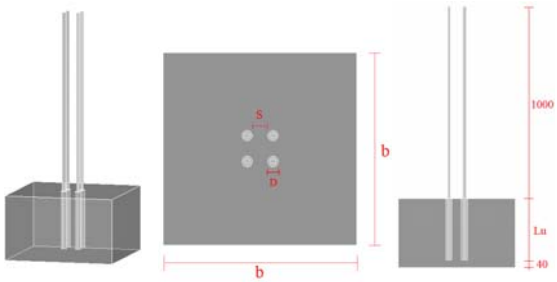

Fig. 4. Specimen Details

Table 3 Dimensions of Specimen

Diameter	b (mm)	Lu (mm)	S (mm)							
			1.5D	**2D**	**2.5D**	**3D**	**3.5D**	**4D**	**4.5D**	**5D**
D16	600	320	48	64	80	96	112	128	144	160
D19	650	380	57	76	95	114	133	152	171	190
D22	750	440	66	88	110	132	154	176	198	220
D25	800	500	75	100	125	150	175	200	225	250
D28	850	560	84	112	140	168	196	224	252	280

III. Results and Discussions

The output in every running process is the stress (S), strain (E), displacement (U), the reaction types (RF, CF), contacts (C), and the parameter of damage (Damage). To address the existing problems, the variable of the output analyzed in this modeling is the stress, strain and fractures/ damage. There are several theories used by ABAQUS to calculate stress, such as Von misses, Tresca, pressure, and the principal stress. The approach used in this research is the primary stress. Max Principal is used to getting the results of the maximum tensile stress, while Min Principal is used to obtaining maximum compressive stress. The data of strain and stress is required to justify the materials to the given loads, whereas the variable of fracture/ damage is used to allow a user in checking which material has been damaged.

1. *Percentage of Damage Specimen Modeling Interaction*

Damage scale of the material is in the 0-1 range; score 0 indicates that the material has not damaged. If the damage scale is more than 0, it means that the material has fractured. The higher the score, the higher the damage that occurs in the material. The damage percentage of the number of e[illegible] t d

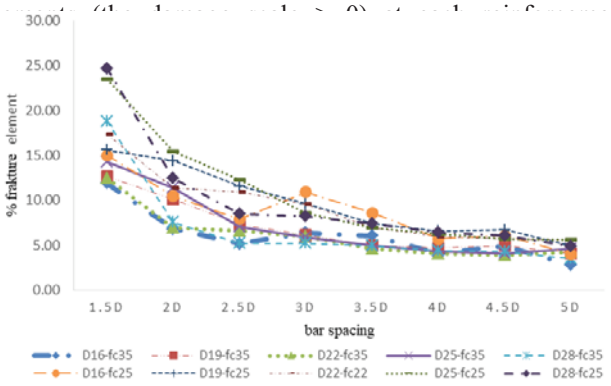

Fig. 5. Damage Percentage of Concrete to Reinforcement Distances

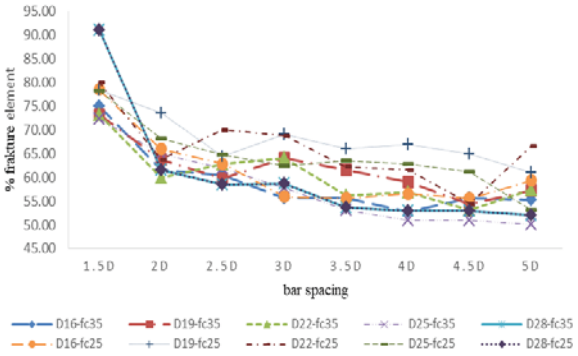

Fig. 6. Damage Percentage of Grouting to Reinforcement Distances

2. *Failure Pattern of Specimen*

Failure pattern of the overall specimens used to determine the minimum reinforcement distance. The minimum length is required to avoid excess or massive damage to the sample. The specimen which its failure pattern is not contacted within the reinforcement distance is determined as minimum reinforcement distance.

Failure Pattern of D16 Specimen

Fig.7 and Fig. 8 show a failure pattern which occurred on specimens D16 with 3.5D and 4D distances. The failure pattern occurred in samples D16-4D shows the reduction of the elements which commit the damage in numbers and also in scale.

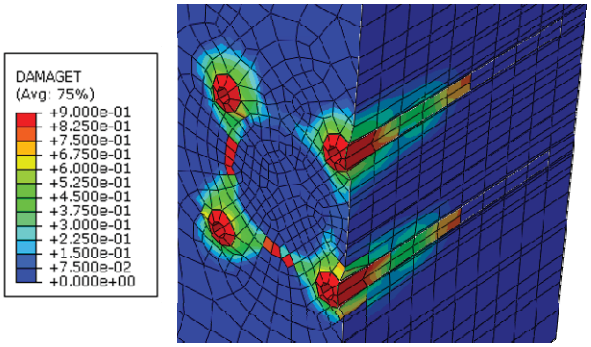

(a). f_c' 25 MPa

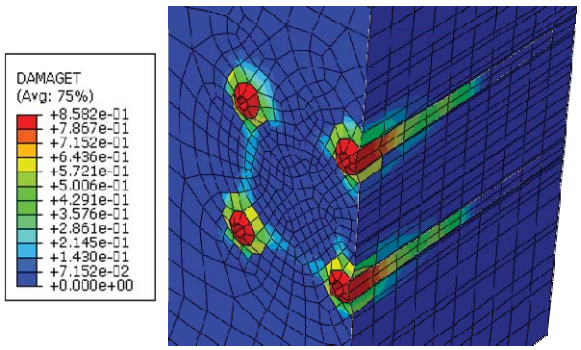

(b). f_c' 35 MPa

Fig. 7. Visualization of Parameter on Damage Tensile on Specimens D16-3.5D: (a) fc25, (b) fc35

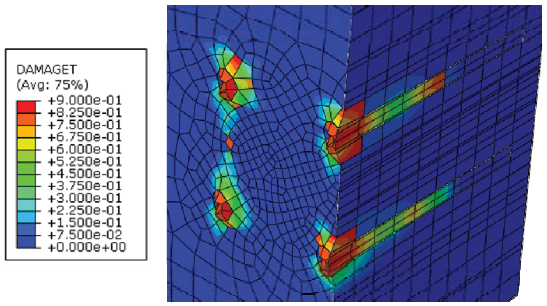

(a). f_c' 25 MPa

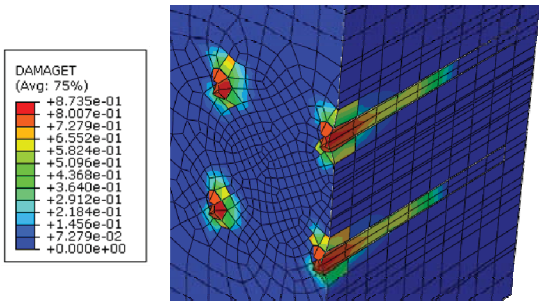

(b). f_c' 35 MPa

Fig. 8. Visualization of Parameter on Damage Tensile on Specimens D16-4D: (a) fc' 25 MPa, (b) fc' 35 MPa

Failure Pattern D19 Specimen

The pattern of failure on D19-3.5D (Fig. 9) shows the direction of cracks is still contacted with the reinforcement distance. While at a distance of 4D (Fig. 10) the areas within the reinforcement distances, the failure does not occur.

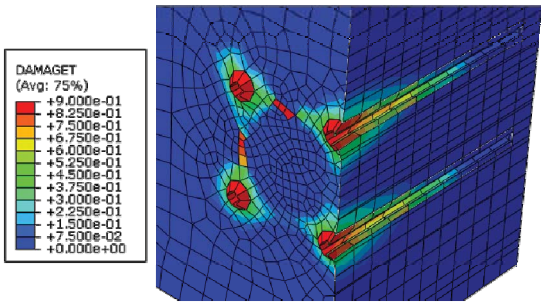

(a). fc' 25 MPa

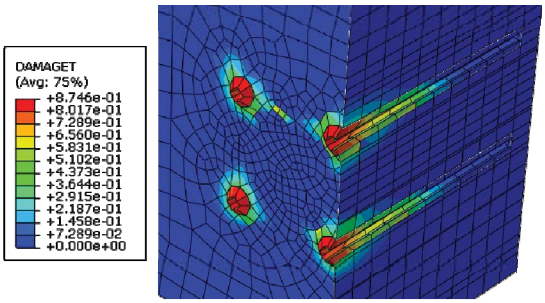

(b). fc' 35 MPa

Fig. 9. Visualization of Parameter on Damage Tensile on Specimens D19-3.5D: (a) fc' 25 MPa, (b) fc' 35 MPa

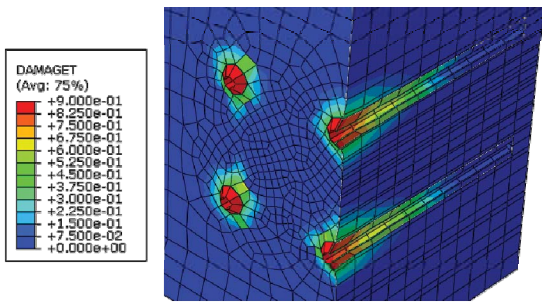

(a). fc' 25 MPa

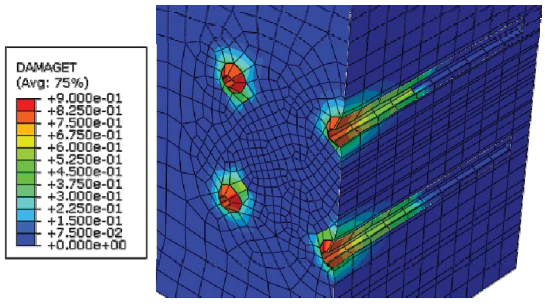

(b). fc' 35 MPa

Fig. 10. Visualization of Parameter on Damage Tensile on Specimens D19-4D: (a) fc' 25MPa, (b) fc' 35 MPa

Failure Pattern of D22 Specimen

The pattern of failure on D22 with 3.5D and 4D distances (Fig. 11 and 12). Based on the figures, failure pattern on D22-4D has fewer damage elements than D22-3.5D.

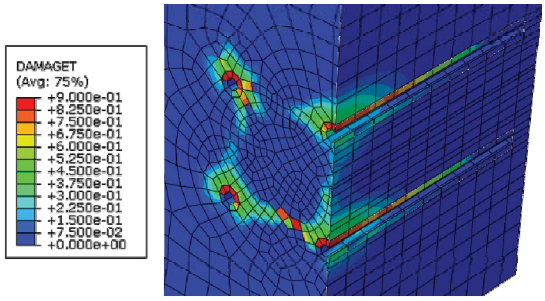

(a). fc' 25 MPa

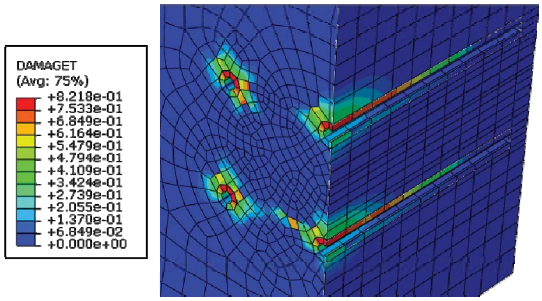

(b). fc' 35 MPa

Fig. 11. Visualization of Max Principal Stress on Specimens D22-3.5D: (a) fc' 25 MPa, (b) fc' 35 MPa

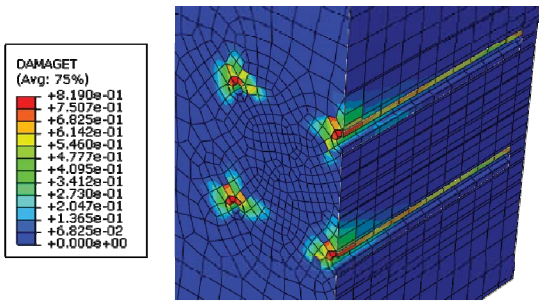

(a). fc' 25 MPa

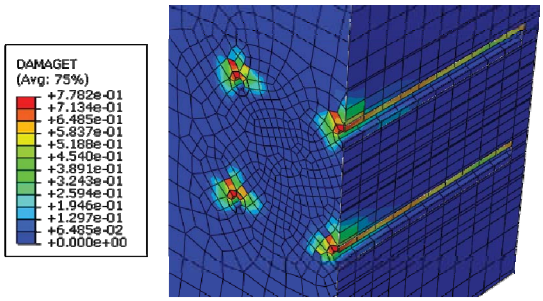

(b). fc' 35 MPa

Fig. 12. Visualization of Parameter on Damage Tensile on Specimens D22-4D: (a) fc' 25 MPa, (b) fc' 35 MPa

Failure Pattern of D25 Specimen

Fig. 13 and Fig. 14 show the failure pattern on specimens D25 with 3.5D and 4D distances. The failure pattern on D25-4D shows the reduction of the damage in numbers and also in scale.

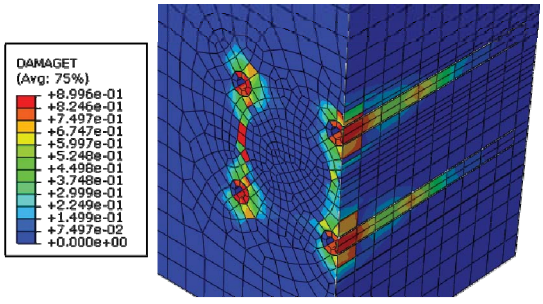

(a). fc' 25 MPa

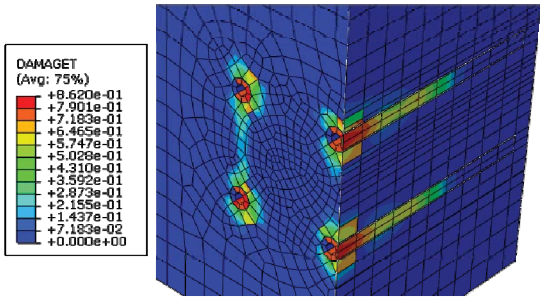

(b). fc' 35 MPa

Fig. 13. Visualization of Parameter on Damage Tensile on Specimens D25-3.5D: (a) fc' 25 MPa, (b) fc' 35 MPa

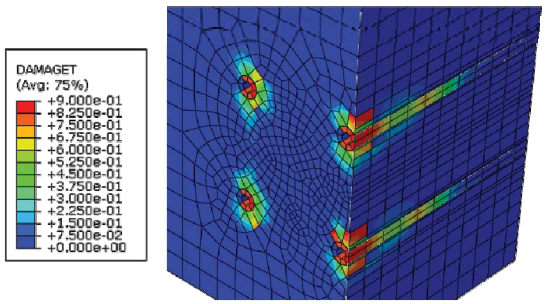

(a). fc' 25 MPa

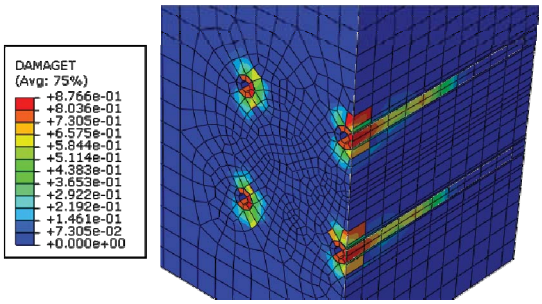

(b). fc' 35 MPa

Fig. 14. Visualization of Parameter on Damage Tensile on Specimens D25-4D: (a) fc' 25 MPa, (b) fc' 35 MPa

Failure Pattern of D28 Specimen

Specimen D28-3.5D commits the failure on the reinforcement distance as shown in Fig. 15, whereas the damage on specimen D28-4D is on the area around bars diameter, but the damaged area is not contacted to each bar (Fig. 16).

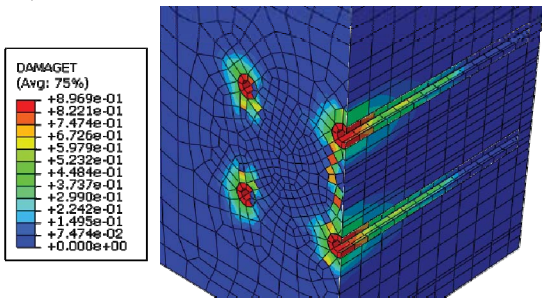

(a). fc' 25 MPa

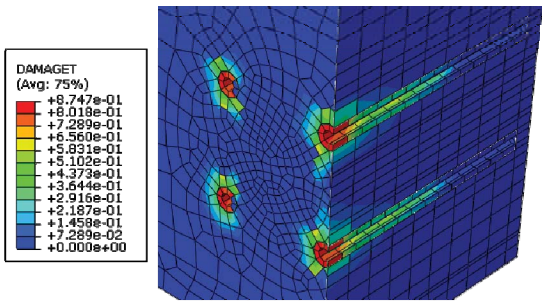

(b). fc' 35 MPa

Fig. 15. Visualization of Parameter on Failure Tensile on Specimens D28-3.5D: (a) fc' 25 MPa, (b) fc' 35 MPa

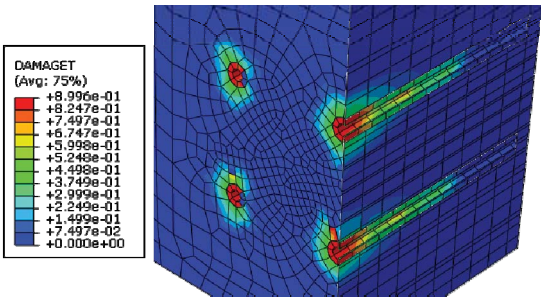

(a). fc' 25 MPa

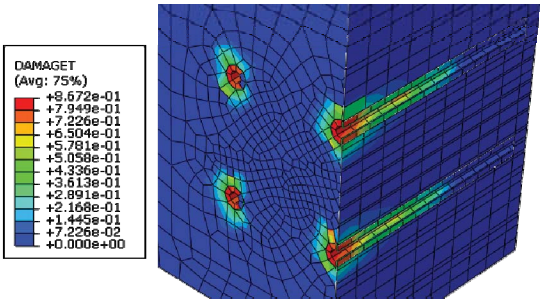

(b). fc' 35 MPa

Fig. 16. Visualization of Parameter on Failure Tensile on Specimens D28-4D: (a) fc' 25 MPa, (b) fc' 35 MPa

IV. CONCLUSIONS

Based on the results of simulation modeling of the pullout test, it can be concluded that:

a. minimum distance (clear distance) of the reinforcement in precast concrete connections using grouting in the pullout test was 4D (D = outer diameter grouting).

b. the failure pattern occurred at a distance of 1.5D-3.5D was a form of cracks between the reinforcement distances on the concrete surface.

While the damage scheme at a distance of 4D-5D was a fracture on some parts of the concrete surface and grouting, but there were no fractures within the reinforcement distances. The wider the reinforcement distances, the less the damage scale and also the fewer damage elements.

V. ACKNOWLEDGMENTS

Thank the Center of Research and Community Service of the Ministry of Higher Education who gave the research grant.

REFERENCE

[1] C. S. Dong, Y.H.; Jaillon, L.; Chu, P.; Poon, "Comparing carbon emissions of precast and cast-in-situ construction methods—A case study of high-rise private building," *Constr. Build. Mater.*, vol. 99, no. November, pp. 39–53, 2015.

[2] S.-J. C. Jong-Pil Won, Hyoung-Ho Kim, Su-Jin Lee, "Carbon reduction of precast concrete under the marine environment," *Constr. Build. Mater.*, vol. 74, no. January, pp. 118–123, 2015.

[3] A. F. F. R. A. Rosyidah, "THE DEVELOPMENT LENGTH OF STEEL BARS FOR PRECAST," 2016.

[4] Q. Yan, T. Chen, and Z. Xie, "Seismic experimental study on a precast concrete beam-column connection with grout sleeves," *Eng. Struct.*, vol. 155, pp. 330–344, 2018.

[5] Z. Lu, Z. Wang, J. Li, and B. Huang, "Studies on seismic performance of precast concrete columns with grouted splice sleeve," *Appl. Sci.*, vol. 7, no. 6, 2017.

[6] A. B. Abd Rahman, M. Mahdinezhad, I. S. Ibrahim, and R. N. Mohamed, "Bond stress in grouted spiral connectors," *J. Teknol. (Sciences Eng.*, vol. 77, no. 16, pp. 49–57, 2015.

[7] K. P. Steuck, M. O. Eberhard, and J. F. Stanton, "Anchorage of large-diameter reinforcing bars in ducts," *ACI Struct. J.*, vol. 106, no. 4, pp. 506–513, 2009.

[8] E. E. Matsumoto, M. C. Waggoner, M. E. Kreger, J. Vogel, and L. Wolf, "Development of a precast concrete bent-cap system," *PCI J.*, vol. 53, no. 3, pp. 74–99, 2008.

[9] T. Jankowiak and T. Lodygowski, "Identification of parameters of concrete damage plasticity constitutive model," *Found. Civ. Environ. ...*, no. 6, pp. 53–69, 2005.

[10] M. Hasan, H. Okuyama, Y. Sato, and T. Ueda, "Stress-Strain Model of Concrete Damaged by Freezing and Thawing Cycles," *J. Adv. Concr. Technol.*, vol. 2, no. 1, pp. 89–99, 2004.

[11] P. Grassl, M. Johansson, and J. Leppänen, "On the Numerical Modelling of Bond for the Failure Analysis of Reinforced Concrete," *Eng. Fract. Mech.*, 2017.

[12] W. Ren, L. H. Sneed, Y. Yang, and R. He, "Numerical Simulation of Prestressed Precast Concrete Bridge Deck Panels Using Damage Plasticity Model," *Int. J. Concr. Struct. Mater.*, vol. 9, no. 1, pp. 45–54, 2015.

[13] M. Ramezani, J. Vilches, and T. Neitzert, "Pull-out behavior of galvanized steel strip in foam concrete," *Int. J. Adv. Struct. Eng.*, vol. 5, no. 1, p. 24, 2013.

[14] P. Akishin, A. Kovalovs, V. Kulakov, and A. Arnautov, "Finite element modelling of slipage between FRP rebar and concrete in pull-out test," *Proc. Int. Conf. „Innovative Mater. Struct. Technol.*, p. 6, 2014.

[15] J. Lubliner, J. Oliver, S. Oller, and E. Oñate, "A plastic-damage model for concrete," *Int. J. Solids Struct.*, vol. 25, no. 3, pp. 299–326, 1989.

[16] G. L. Lee, J., & Fenves, "Plastic-damage model for cyclic loading of concrete structures," *J. Eng. ing Mech.*, vol. 124, no. 8, pp. 892–900, 1998.

[17] S. P. Hibbitt K, Karlsson B, *ABAQUS: Example problems manual*. Hibbitt Karlsson & Sorensen, Inc., USA, 2004.

[18] ABAQUS, *Example problems manual*. Hibbitt Karlsson & Sorensen, Inc., USA, 2004.

[19] Sandor Popovics, "A numerical approach to the complete stress-strain curve of concrete," *Cem. Concr. Res.*, vol. 3, no. 5, pp. 583–599, 1973.